sustainability

MDPI

Article

Reduction of High-Chromium-Containing Wastewater in the Leaching of Pyritic Waste Rocks from Coal Mines

Rodrigo de Almeida Silva [1,*], Marina Paula Secco [2], Jean Carlo Salomé dos Santos Menezes [3], Ivo André Homrich Schneider [4] and Richard Thomas Lermen [1,*]

[1] Postgraduation Program of Civil Engineering, School of Engineering and Applied Sciences, ATITUS Educação, Passo Fundo 99070-220, RS, Brazil
[2] Postgraduate Program in Civil Engineering (PPGEC), Federal University of Rio Grande do Sul (UFRGS), Porto Alegre 90035-190, RS, Brazil
[3] Postgraduate Program in Civil and Environmental Engineering (PPGEng), University of Passo Fundo, Passo Fundo 99052-900, RS, Brazil
[4] Postgraduate Program in Mining, Metallurgical and Materials Engineering (PPGE3M), Federal University of Rio Grande do Sul (UFRGS), Porto Alegre 90130-120, RS, Brazil
* Correspondence: rodrigo.silva@atitus.edu.br (R.d.A.S.); richard.lermen@gmail.com (R.T.L.); Tel.: +55-54-3045-6100 (R.T.L.)

Abstract: Coal is an abundant resource which can be used to produce low-cost energy; however, its usage causes great environmental damage. Before mineral coal can be used, it must be processed to remove coal tailings. These tailings contain pyrite and accumulate in large dumps, presenting significant environmental liabilities, such as acid mine drainage. Another industry that generates environmental liabilities is the chrome-plating industry, mainly because it produces hexavalent chromium (Cr^{6+}) waste. The main aim of this work was to evaluate Cr^{6+} as a reduction agent in trivalent chromium (Cr^{3+}) conversion in the leaching of coal-mine waste containing pyrite. Cr^{3+} is about 100 times less toxic than Cr^{6+} and can be easily removed from industrial effluents by alkaline precipitation. There are several sources of effluents containing Cr^{6+}—a compound which is known worldwide to be toxic, carcinogenic, and mutagenic. A leaching and treatment device was developed and tested for waste treatment. The results indicated that the developed treatment system reduced 100% of Cr^{6+} to Cr^{3+} through pyrite leaching in a Cr^{6+} wastewater sample from the electroplating industry. In addition, the chromium sludge resulting from the treatment process, after calcination, was tested in a ceramic glaze as a pigment and, when compared with an industrial pigment, showed similar mineralogical characteristics.

Keywords: chromium reduction; pyrite oxidation; chromium pigment

Citation: Silva, R.d.A.; Secco, M.P.; Menezes, J.C.S.d.S.; Schneider, I.A.H.; Lermen, R.T. Reduction of High-Chromium-Containing Wastewater in the Leaching of Pyritic Waste Rocks from Coal Mines. *Sustainability* **2022**, *14*, 11814. https://doi.org/10.3390/su141911814

Academic Editors: Chun Zhao, Yunhua Zhu and Hongguang Guo

Received: 16 August 2022
Accepted: 15 September 2022
Published: 20 September 2022

1. Introduction

Many authors have evaluated the environmental impact of using coal to provide electricity, steel, cement, and coal-to-liquid fuels worldwide in terms of waste generation [1–5], acid mine drainage (AMD), and soil, water, and air pollution, in addition to the damage to people's lives [6–9].

In the Brazilian carboniferous regions of Santa Catarina and Paraná, after extraction, coal needs to be processed in order to meet the combustion standards of thermoelectric plants. As a result of the treatment requirements, approximately 60% of the total amount of coal produced becomes solid waste, of which between 10% and 65% consists of pyrite, which must be discharged in waste deposits [10].

Pyrite (FeS_2) is a major natural sulfate mineral associated with hydrothermal mineral formation, ore deposits, and sedimentary media in anoxic conditions [11–13]. Pyrite is considered an industrial waste because it is responsible for acid mine drainage (AMD), which occurs as a result of the natural oxidation of pyrite in contact with water and oxygen.

AMD is recognized as one of the most serious environmental problems in the mining industry due to the high acidity of the drainage water (it has a pH less than 3.5) and its high contents of soluble metals and sulfates [14–17]. However, pyrite can be a valuable ore mineral in certain contexts [18].

The natural process of pyrite oxidation occurs in a number of stages. First, reaction (1) shows the oxidation of pyrite with molecular oxygen in the presence of excess water at neutral pH; in this case, Fe^{2+} is released and sulfate acidity leads to a pH decrease. Then, molecular oxygen or bacterial action convert the Fe^{2+} into Fe^{3+} (reaction (2)) [19–21]. The overall reaction for pyrite oxidation (reactions (1)–(3)) is summarized in reaction (4). Reaction (5) shows the complete oxidation of pyrite, in which iron acts as the oxidizing agent. In the presence of water and oxygen, global pyrite oxidation is represented by reaction (6).

$$FeS_2 + \frac{7}{2}O_2 + H_2O \leftrightarrow Fe^{2+} + 2(SO_4)^{2-} + 2H^+ \quad (1)$$

$$Fe^{2+} + \frac{1}{2}O_2 + H^+ \leftrightarrow Fe^{3+} + \frac{1}{2}H_2O \quad (2)$$

$$Fe^{3+} + 3H_2O \leftrightarrow Fe(OH)_3 + 3H^+ \quad (3)$$

$$FeS_2 + \frac{15}{2}O_2 + \frac{7}{2}H_2O \leftrightarrow Fe(OH)_3 + 2(SO_4)^{2-} + 4H^+ \quad (4)$$

$$FeS_2 + 14Fe^{3+} + 8H_2O \leftrightarrow 15Fe^{2+} + 2(SO_4)^{2-} + 16H^+ \quad (5)$$

$$FeS_2 + \frac{15}{4}O_2 + \frac{1}{2}H_2O \leftrightarrow Fe^{3+} + 2(SO_4)^{2-} + H^+ \quad (6)$$

Pyrite oxidation is a complex reaction; if a gap exists between the top of the valence band and the bottom of the conduction band, this is referred to simply as the band gap [22]. Rimstidt [23] describes pyrite oxidation in three distinct steps: in the first step, a cathodic reaction is generated by the transfer of electrons from pyrite surfaces to aqueous oxidant species, usually O_2 or Fe^{3+}; in the second step, charge is transported from the anodic site of the reaction to replace the electrons lost from the cathodic site; in the last step, at the anodic site, the oxygen atoms of water molecules interact with sulfur atoms to create oxidized sulfoxide species [24]. Metal sulfides can be used as cathodes or anodes, especially natural FeS_2 ore (pyrite), because of their high electron-change capacities ($4e^-/FeS_2$) and low costs (~USD 0.5 per kg) [25,26].

Several researchers have already studied the reduction of hexavalent chromium (Cr^{6+}) under analytical and/or industrial conditions in the leaching of pyrite [27–31]. Chromium reduction occurs through the action of pyrite, which acts as a reducing agent, transforming hexavalent chromium into trivalent chromium. This process can be used to treat industrial effluents with hexavalent chromium; it is a treatment technique that is simple, effective, and economical for the treatment of wastewater.

Benincasa et al. [28] and Kantar et al. [32] studied the reaction between Cr^{6+} and pyrite. The researchers evaluated the effects of pH and different Cr^{6+} concentrations on chromium-reduction behavior. The results demonstrated that Cr^{6+} reduction by pyrite decreased with increasing solution pH and Cr^{6+} concentration. The decrease in Cr^{6+} removal with increasing Cr^{6+} concentration indicated that there was a limited number of surface reactive regions in the pyrite; that is, with excess surface regions, Cr^{6+} adsorption onto pyrite surfaces regulated the overall rate of Cr removal, leading to first-order reaction kinetics. It can also be stated that Cr^{6+} oxidatively dissolved the pyrite surface, releasing ferrous iron and sulfates into the reaction solution as the reaction progressed [31]. Cr^{6+} reduction is significant at pH < 2.3, and the reduction of Cr^{6+} to Cr^{3+} involves the oxidation of Fe and S_2, according to reaction (7). Finally, all pyrite particles at acidic pH show variable Cr contents on their surfaces.

$$2FeS_2 + 5(Cr_2O_7)^{2-} + 32H^+ \leftrightarrow 2Fe(OH)_3 + 4(SO_4)^{2-} + 10Cr^{3+} + 13H_2O \quad (7)$$

Chromium has special importance as the fifth metallic chemical element, after iron, aluminum, manganese, and copper. It is the main constituent of chromite, which is considered one of the most important industrial minerals in the world, its applications covering a range of industrial processes, metallic and non-metallic [33]. Resources of chromium derive from around 12 billion tons of chromite—a quantity sufficient to meet conceivable demand for centuries. These resources are concentrated in Kazakhstan, Southern Africa, Russia, and India [34–36]. Chromium occurs in 82 different types of and exclusively in ultramafic igneous rocks, but only the chromite type is mined commercially. Chromite varies widely in composition according to the chemical formula (Mg, Fe^{2+})(Cr, Al, Fe^{3+})$2O_4$, the varying proportions depending on the deposits [37].

Industrial uses of chromium include ferrous and nonferrous alloy production, chromium plating, corrosion control, metal finishing, and incorporation into pigments, tanning compounds, wood preservatives, cement kilns, and glass-tank regenerators, among other uses [38–42].

Generation of residues is the main problem regarding the industrial application of chromium. Chromium is a transition metal with atomic number 24 and can be found in several oxidation states; however, the most common states found in natural environments are Cr^{6+} and Cr^{3+} [43,44]. Cr^{3+} is a stable form and 100 times less toxic than Cr^{6+} and is essential to humans in the metabolism of insulin. On the other hand, Cr^{6+} is a strong oxidizing agent and a skin and mucous membrane irritant; it also produces allergic reactions, such as eczema, in addition to respiratory disorders, kidney circulation problems, lung cancer, and gastrointestinal distress [43–46].

Wastewater-containing Cr^{6+} is produced by different industrial processes, such as metal plating, pigment and dye production, surface coating, leather tanning, and corrosion inhibitor manufacturing [32,47–49]. The reduction of Cr^{6+} to Cr^{3+} and the formation of insoluble Cr^{3+} precipitates are essential steps in the treatment of water and soil contaminated with Cr^{6+} [18]. Generally, the treatment of Cr^{6+} effluent (reduction of Cr^{6+} to Cr^{3+}) is carried out using iron salts, sulfur compounds, metal particles, and precipitation by pH adjustment. At the end of the treatment process, an insoluble chromium hydroxide [$Cr(OH)_3$] is produced [50–53]. However, in all cases, treatment produces large amounts of sludge that presents difficulties in terms of management, transportation, and costs associated with final disposal in landfill, in addition to the potential leaching of hazardous waste during storage [54–56].

The development of pigments with low-cost raw materials has been a longstanding industrial aim and is required by the ceramic sector to increase market competitiveness [57]. Additionally, it has been reported by Pelino [58] and Garcia-Valles et al. [59] that the inerting of hazardous waste in ceramic matrices seems more suitable due to the technologies of production, with high-temperature vitrification converting hazardous waste into non-hazardous glass or glass–ceramic materials.

Many surveys have been developed regarding the recovery of chromium for use as a ceramic pigment from the waste produced in the chrome-plating process. The solid waste residues from a metallurgical plant containing high amounts of Cr^{3+} have been applied in ceramic glazes [60]. Costa et al. [61] developed a spinel pigment by a combination of two different sludges generated from Cr/Ni plating and Fe-rich galvanizing sludge generated during steel wiredrawing. Berry et al. [62] evaluated the possibility of producing chromium commercial pigment using Cr^{3+} tanned-leather shavings as a source of chromium.

In the present study, the aim was to evaluate the possibility of treating two hazardous materials (high-chromium-containing wastewater from the electroplating industry and pyrite derived from coal mining) together to generate a new product (chromium pigment).

The chromium reduction system was evaluated according to variations in oxidation–reduction potential (ORP), Cr^{6+} concentration, and changes in pyrite particle size. After calcination, the solid material resulting from the filtration process (chromium sludge) was characterized by X-ray diffraction (XRD), X-ray fluorescence (FRX), and particle size and colorimetric parameters and applied in a ceramic glaze as a pigment. The advantages of

the chromium pigment generated from the waste are its low cost compared to industrial chromium pigment and the significantly minimized environmental impacts and costs of the generators required for the chromium and pyrite waste processing. Regarding the disadvantages of this pigment, it can be said that adjustments to pigment composition must be carried out to obtain different colors, the calcination process can oxidize Cr^{3+} to Cr^{6+} [63], and a large amount of chromium waste is needed to obtain a small amount of pigment (for example, 100 L of high-chromium-containing wastewater generates approximately 350 g of pigment).

2. Materials and Methods

2.1. Materials

Pyrite concentrate was obtained by the jigging of coal tailings from Cambuí Mine, Paraná, Brazil—the same deposits that were characterized by Menezes et al. [64]. The material is composed of 65% FeS_2, with around 35% pyritic sulfur compounds that can be used as reductant agents. Furthermore, this material was analyzed for specific density, apparent density, particle size, and pore space. Figure 1 shows the fractions of pyrite that were used as reductant agents in the lixiviation column system.

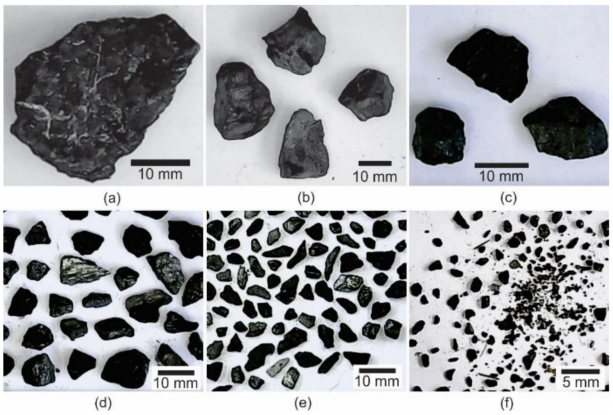

Figure 1. Pyrite fractions distributions retained in the sieve: (**a**) 9.5 mm, (**b**) 6.3 mm, (**c**) 4.75 mm, (**d**) 2.36 mm, (**e**) 1.18 mm, and (**f**) the bottom.

A high-chromium-containing wastewater sample was collected from the tank used in the current treatment carried out in the electroplating industry. Nowadays, this small industry produces bolts, clamps, metal clips, and other materials used in agricultural machines and generates around 300 L/week of chromium effluent. After proper treatment, the metallic sludge is finally discharged at a high cost, besides the considerable wastage of material. The sample obtained contained a Cr^{6+} concentration of 0.0096 M and had a pH of 2.39.

2.2. Experimental Equipment and Procedure

The leaching column system consisted of a column in a polyvinyl chloride tube that was 700 mm in height and 150 mm in diameter, and the base of the column was installed with a stopcock for flow control. Ninety percent of the column was used as a leaching bed and was filled up with pyrite waste, 30% of this volume being empty space that was covered with effluent and 10% of the leaching bed not being covered to permit contact between pyrite surfaces and improve pyrite oxidation. The retention time between the wastewater and the leaching bed was 3.4 min. The maximum capacities for the leaching device developed were 15 kg of pyrite added to the leach cell and 100 L of high-chromium-containing wastewater in the reservoir.

Recirculation was carried out with a submerged pump at a flow rate of 72 L/h. One-hundred liters (L) of chromium wastewater was percolated through the system until the total reduction of Cr^{+6} to Cr^{3+}. The initial pH value was 2.7 $\pm$ 0.1 and the solid–liquid ratio

was 150 g/L. A schematic drawing of the leaching column system is shown in Figure 2a. After 36 h of recirculation, the pH of the solution was adjusted to 8.5–8.7 with sodium hydroxide (99% of purity) to form the sludge (Figure 2c), which was removed by filtration. All experiments were performed at room temperature (25 °C), and three repetitions of the experiments were performed.

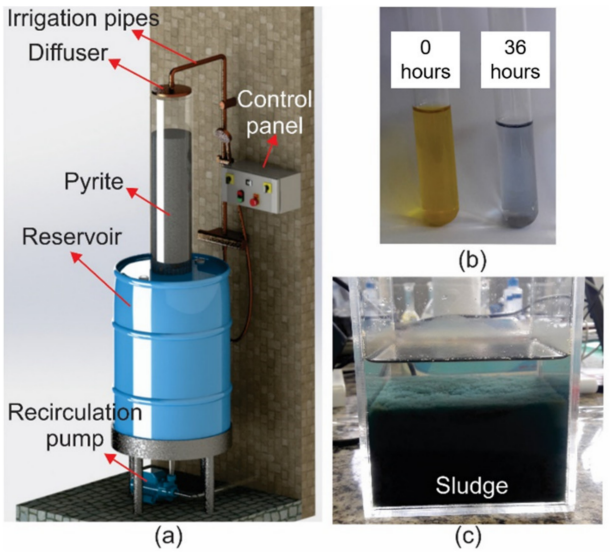

Figure 2. (**a**) Schematic drawing of the chrome treatment system—leaching column device. (**b**) Color change of effluent in the reduction process. (**c**) Sludge in the wastewater treatment.

To evaluate the pyrite-reduction capacity, oxidation–reduction potential (ORP) and Cr^{6+} concentration were measured. The wastewater solution had a pH between 2.0 and 2.7, which was naturally maintained in this range by pyrite dissolution, because this reaction generates sulfuric acid by sulfur oxidation. Figure 2b shows the wastewater color change after 36 h of the reduction process. Furthermore, changes in pyrite particle size were determined to evaluate the degradation of pyrite by leaching.

As a result of the filtration process, 390 g of solid material was dried, ground, and calcined at 1100 °C for 2 h, following the procedure used by Ozel and Turan [65]. A calcined sample was characterized by X-ray diffraction (XRD), X-ray fluorescence (FRX), particle size, and colorimetric parameters. A powder with particles of sizes less than 75 µm was called Chromium Sludge Pigment (ChSlPi) and was compared with Industrial Pigment (InPi) in terms of its granulometric, mineralogical, and chemical characteristics. Both pigments were treated under the same conditions and sequentially applied in ceramic glazes. The hexavalent chromium wastewater, before and after pyrite treatment, was characterized according to environmental legal rules, and the metal contents were evaluated by colorimetric methods [66]. All analyses followed the procedures described in the Standard Method for the Examination of Water and Wastewater [67].

2.3. XRD Methodology

In order to identify the crystalline phases by XRD, a SHIMADZO XRD 6100 diffractometer was used, with CuKa (l = 1.5418 Å) radiation, operating at 40 kV and 30 mA. The data collection was carried out with a step interval of 0.02° and a step time duration of 0.6 (s), in the 2θ range of 4 to 80°. The data collections were identified using HighScore Plus software for ICDD-pattern indexing. Amounts of crystalline phases were determined by the Rietveld method.

2.4. XRF Methodology

The chemical compositions of the materials (ChSlPi and InPi) were analyzed by X-ray fluorescence with dispersive energy (EDXRF) using a Shimadzu EDX-7000 spectrometer. The analysis was performed by the Solid Fuels Laboratory (SATC—Criciúma/SC).

2.5. Particle Size

The particle-size analyses were carried out by LASER diffraction, in water, according to the Fraunhofer method, using a Bettersizer S2-WD device. Particle-size analysis was performed by the Laboratório Central de Equipamentos Multiusuários—Cemulti, Passo Fundo/RS.

2.6. Colorimetric Parameters

The colors of the sample (ChSlPi) and industrial pigment (InPi) were characterized by differential colorimetry (DL*a*b) using the colorimetric parameters L*a*b. Figure 3a show the brown–red Industrial Pigment (Industrial Pigment—InPi) and Figure 3b shows the brown pigment (Chromium Sludge Pigment—ChSlPi). The pastille sample was made with 2 g of sample compacted with 74 N/cm^2. The color was evaluated with a Minolta 2600d spectropolarimeter in the Mineral Processing Laboratory (LAPROM), Federal University of Rio Grande do Sul, Brazil.

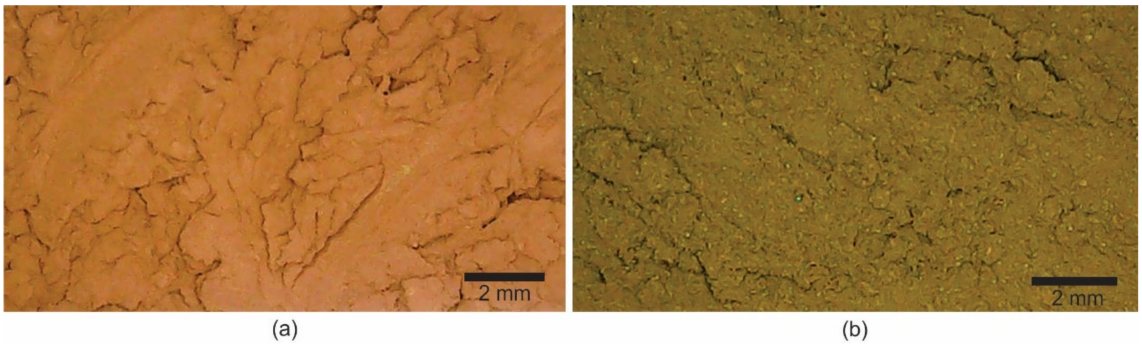

Figure 3. (**a**) Brown–red industrial pigment (InPi). (**b**) Brown chromium sludge pigment (ChSlPi).

3. Results and Discussion

The chromium reduction system was evaluated for wastewater effluent to analyze the changes in the sizes of particle and chemicals variations in ORP potential and Cr^{6+} concentration. The leaching promotes the consumption of fine particles of less than 2.36 mm. After cycle tests, the particle sizes of pyrite showing soft density increased by around 3% and porous space increased by around 8.5%, in addition to a decrease in the apparent density of around 10%, probably as a result of the dissolution of fine particles. These results are shown in Figure 4.

Another important result obtained with this controlled system was an ORP evaluation for chromium reduction by pyrite oxidation. The ORP value for the Cr^{6+} solution before leaching was 624 mV, and this was reduced to 355 mV after 36 h of recirculation. Figure 5 show the reduction percentages of Cr^{6+} and Cr^{3+} as a function of leaching time. It can be observed that, over approximately 480 min of leaching time, the Cr^{6+} and Cr^{3+} concentrations were practically the same and, as expected, when the amount of Cr^{6+} decreased, the amount of Cr^{3+} increased. In addition, the total amount of chromium remained constant.

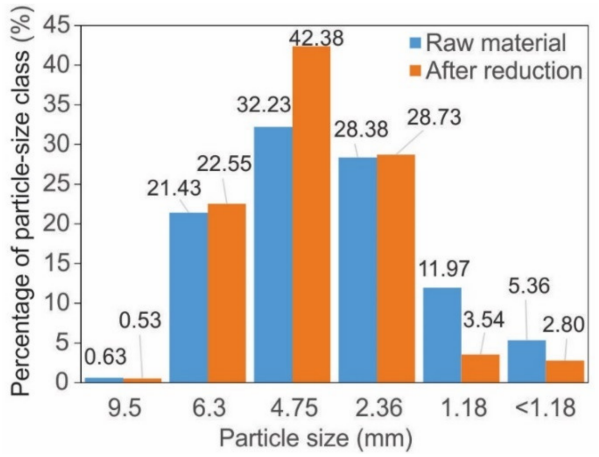

Figure 4. Changes in the particle size behavior of the pyrite concentrate after chromium reduction.

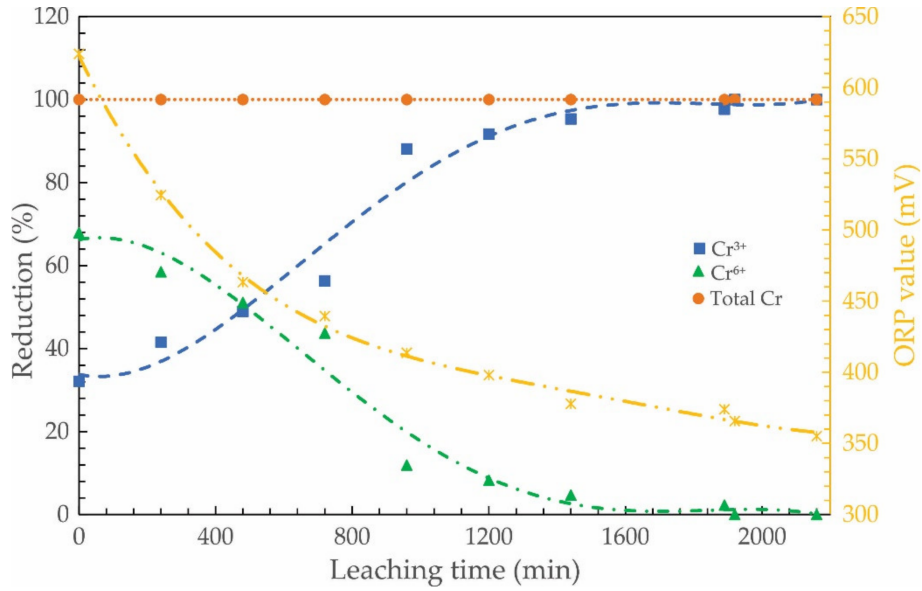

Figure 5. ORP, Cr^{3+}, Cr^{6+}, and Total Cr concentration (%) as a function of leaching time.

The behavior of chromium reduction kinetics can be described by fourth-order polynomial regression for the leaching time interval and the conditions used in the experiment. Equations (8) and (9) show the regressions for the reduction of Cr^{6+} and Cr^{3+}, respectively:

$$Cr^{6+}reduction\ (\%) = -2{\cdot}10^{-11}{\cdot}x^4 + 10^{-7}{\cdot}x^3 - 0.0002{\cdot}x^2 + 0.0187{\cdot}x + 66.4 \quad (8)$$

$$Cr^{3+}reduction\ (\%) = 2{\cdot}10^{-11}{\cdot}x^4 - 10^{-7}{\cdot}x^3 + 0.0002{\cdot}x^2 - 0.02{\cdot}x + 33.7 \quad (9)$$

where x is the leaching time. The coefficients of determination for Equations (8) and (9) were $R^2 = 0.975$ and $R^2 = 0.9776$, respectively.

The color change of solutions can be seen in Figure 6, in which the orange solution (Cr^{6+}) turned green (Cr^{3+}). It is very important to report that the chromium reduction by pyrite leaching depends on the surface oxidation of pyrite and on the pH of the solution [68].

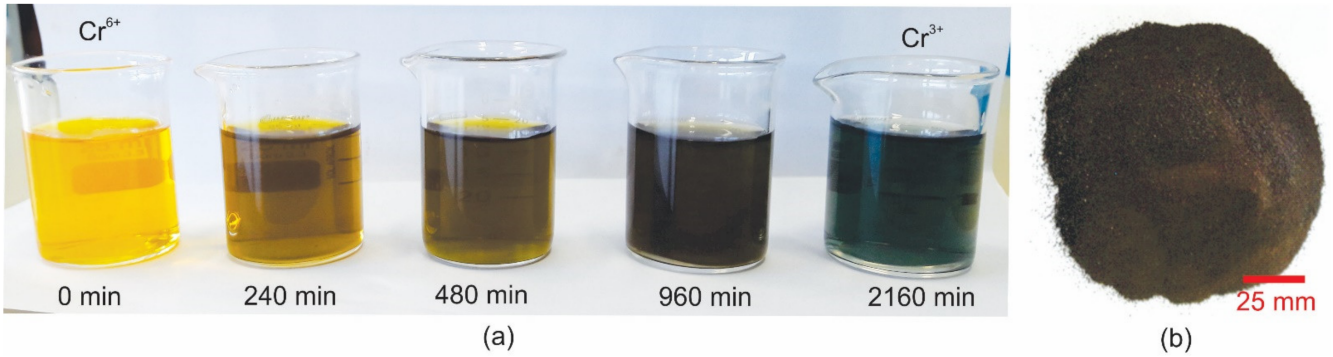

Figure 6. (**a**) Color change of Cr^{6+} in chromium reduction. (**b**) Calcined sample.

Color change is related to a change in 3d orbital electronic levels and ligand field splitting, hence the change in absorption spectra and the resulting color. If the ligands change, usually the light–matter interaction energy also changes (ΔE_{elec}). In case of Cr^{3+} color change, the excitation of an electron from the lower 3d orbital to a higher 3d orbital in the hexaamminechromium (III) complex ion occurs. Regarding Cr^{6+}, the orange dichromate (VI) ions form an equilibrium and one species dominates, depending on the pH of the solution. Change in the pH of the solution (Cr^{6+}) does not result in a change of oxidation state, but the electronic environments of the central chromium ions are changed such that they have different UV–visible absorption spectra and different field-splitting ΔE_{elec} values, resulting in color variations in the Cr^{6+} solution [69].

According to the ASTM D7348-21 standard [70], the pigment had a 3.8% of loss ignition. The sample calcined (Figure 6b) was analyzed to identify the chemical composition and the mineral phases formed. Figures 7 and 8 show the diffractograms for the InPi and ChSlPi pigments, respectively.

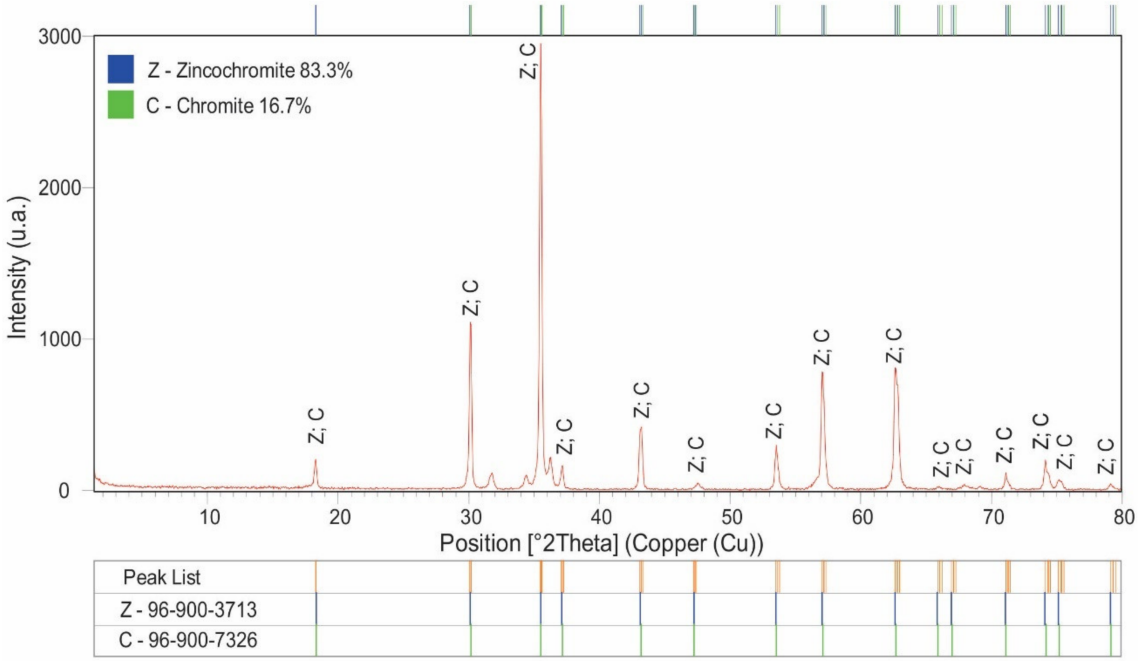

Figure 7. Diffractogram of the Industrial Pigment (InPi).

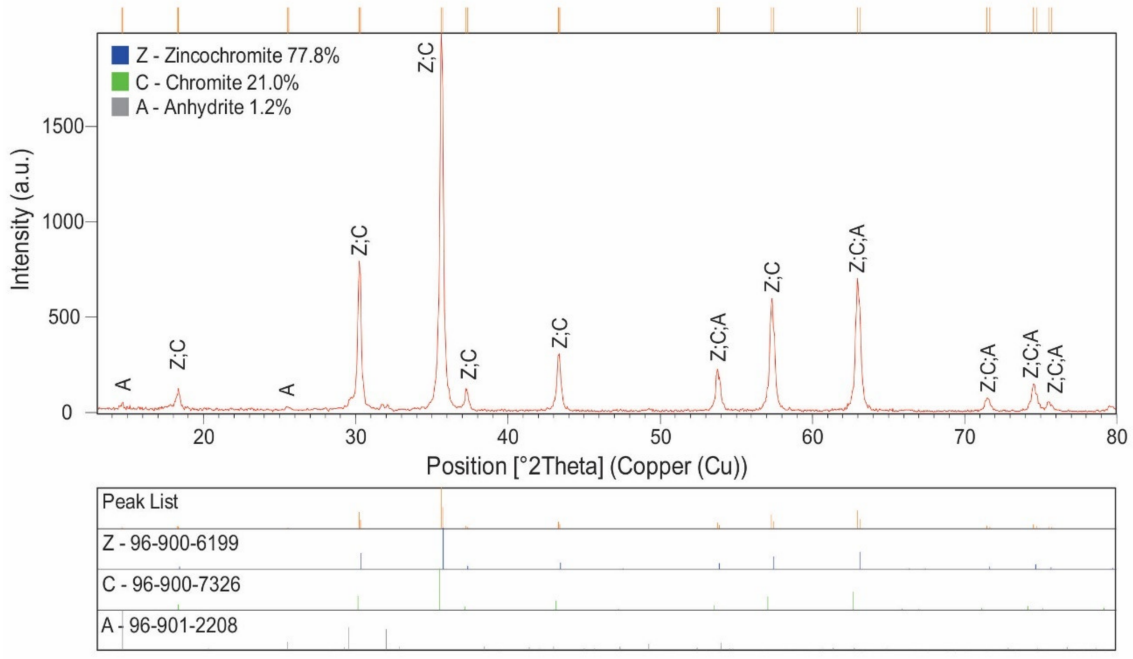

Figure 8. Diffractogram of the Chromium Sludge Pigment (ChSlPi).

The diffraction patterns confirmed zincochromite and chromite as majority phases in the two samples. InPi showed a more defined phase than the treatment with coal waste concentrate (pyrite), but the treatment system was effective in converting two wastes into one material with mineralogical phases very similar to the raw industrial material. On the other hand, the chemical composition (Table 1) between the two samples (InPi and ChSlPi) showed differences, mainly concerning chromium, iron, and zinc contents. It can be said that the chromium and zinc came from the wastewater galvanization and that the iron came from the pyrite dissolution.

Table 1. Chemical compositions of the materials.

Composition	Cr_2O_3	Fe_2O_3	ZnO	SiO_2	SO_3	CaO	CuO	Others
ChSlPi	50.45	13.64	30.19	0.36	3.46	1.38	0.06	0.46
InPi	29.32	28.99	40.89	0.35	0.32	0.06	0.06	0.02

Large amounts of chromium could be observed in both pigments. According to Liao et al. [71] and Li et al. [72], the amount of chromium contained in a pigment, when applied in the sintering of ceramic glaze, has no influence on toxicity, because glass–ceramic materials form spinel structures and residual glass successfully immobilizes Cr.

To evaluate the differences in particle-size distribution between InPi and ChSlPi samples, granulometric analyses were performed. The results indicated that ChSlPi had bigger particles than InPi, which can result in poor dispersion in pigment applications in ceramics. This dispersion problem can be solved with wet grinding media to achieve a suitable particle size. The results are shown in Figure 9.

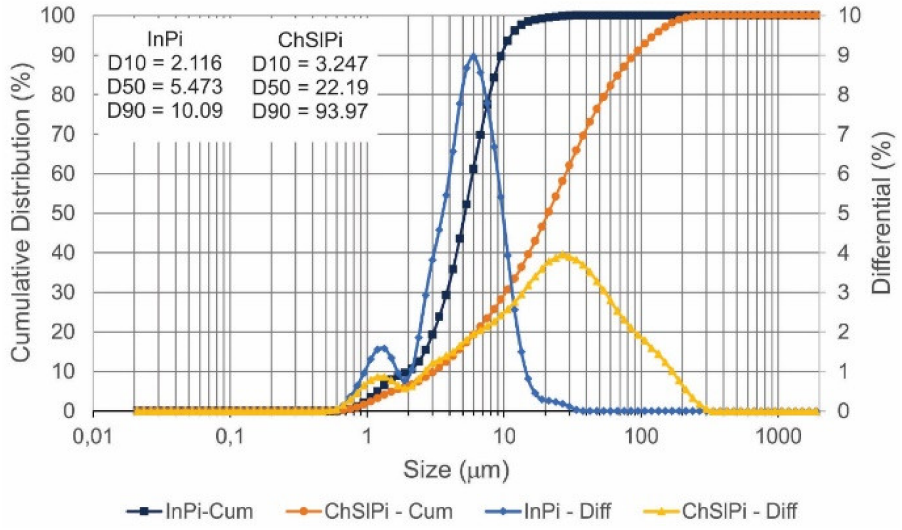

Figure 9. Particle-size distributions for InPi and ChSlPi.

The two pigment samples were compared with respect to their color behavior. The colorimetric behavior of the two samples pigments obtained from wastewater treatment were evaluated (Table 2).

Table 2. Colorimetric parameters.

Pigment Type	L*	a*	b*	$DE_{L^*a^*b^*}$
InPi	30.61	16.50	10.80	0.00
ChSlPi	28.29	10.10	12.83	25.24

Results for CIE L*a*b* and $DE_{L^*a^*b^*}$ represent color differences; thus, the InPi is lighter in color. Parameter a* reveals that it is redder; b* reveals that it is less yellow. The global color difference is strong ($DE_{L^*a^*b^*}$); however, the color differences above 1.5 can be seen by the human eye [73,74]. On the other hand, the reflection of the light demonstrates the similarity of InPi and ChSlPi when the curve shapes are compared. The percentages of reflectance are in the same region of the spectrum, around 650 nm. Figure 10 shows the percentage reflectance as a function of wavelength in the visible range for InPi and ChSlPi. An adjustment to the chemical composition could be made to increase the similarity between InPi and ChSlPi.

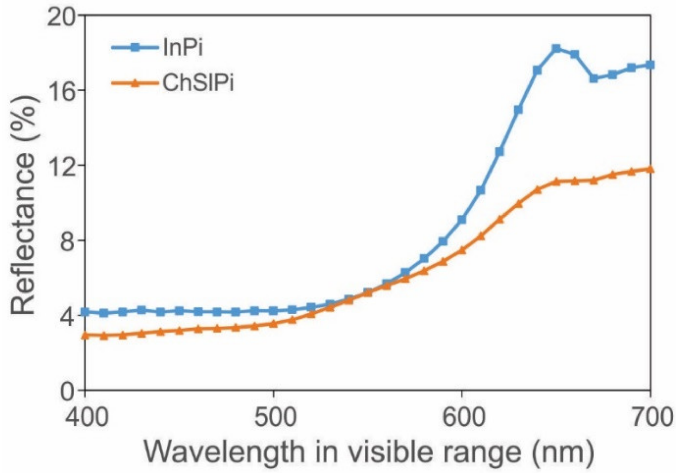

Figure 10. Percentage reflectance curves for InPi and ChSlPi.

The brown–red pigment derived from sludge was submitted to industrial testing in a ceramic factory (Figure 11). Firstly, the brown–red pigment was wet-ground for 10 min with a ball ceramic mill and, to improve the dispersion powder, a dispersant solution was added. The pigment was mixed with 1 Wt% and 5 Wt% with transparent glazes as flux. The mix was homogenized in an eccentric mill for 5 min and applied to ceramic tiles as a surface glaze. The tiles were heated inside a kiln at 1050 °C for 5 min. The methods used to color the ceramic material and determine the composition of the industrial pigment were described by Marcello et al. [75]. It is important to note that the procedure used to implement ChSlPi in the ceramic material was the same as that used to implement the commercial pigment.

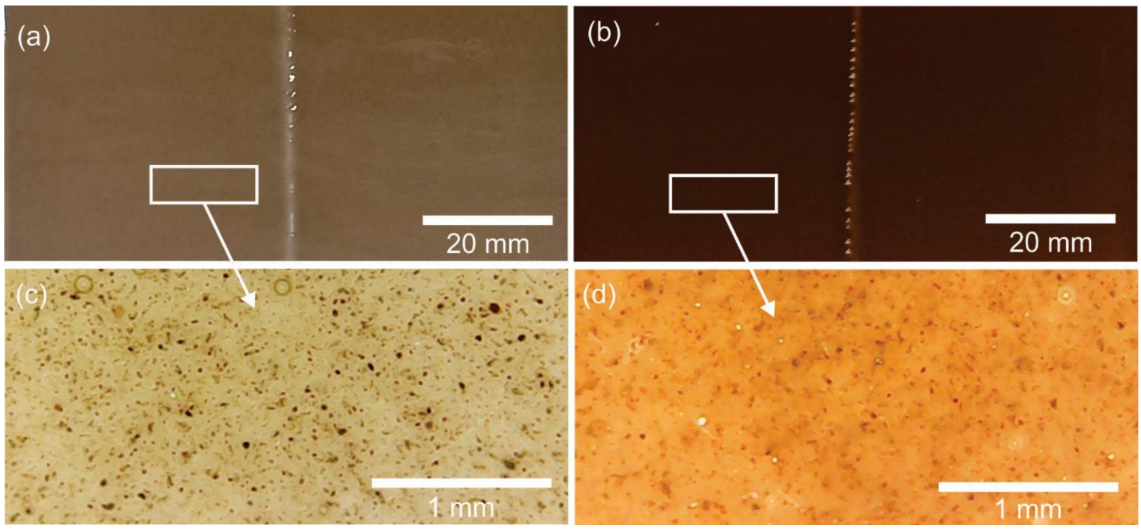

Figure 11. Ceramic tiles painted with (**a**) 1 Wt% and (**b**) 5 Wt% ChSlP. (**c**,**d**) Enlarged images.

Regarding compliance with the environmental rules, the chromium wastewater and treated wastewater were characterized in terms of metal contents, pH, total solids, turbidity, colour haze, and conductivity (Table 3). The results showed that the leaching system treatment was able to reduce all of the Cr^{6+} to Cr^{3+} given the replacement of the conventional reduction system with sodium metabisulfite; in addition, it was not necessary to change the subsequent steps with pH adjustment and solid–liquid separation. After treatment with pyrite, the chromium wastewater was found to satisfy the Brazilian environmental legislation for wastewater disposal.

Table 3. Chemical compositions before and after wastewater treatment.

Parameter	Wastewater	Treated Wastewater	Brazilian Standards CONAMA 430/2011
Trivalent chromium (mg/L)	236.90	0.80	1.00
Hexavalent chromium (mg/L)	500.00	ND	0.10
Total iron (mg/L)	16.20	1.80	15.00
Zinc (mg/L)	210.50	ND	5.00
Manganese (mg/L)	3.40	0.30	1.00
Total solids (mg/L)	11,240.00	0.30	-
Turbidity (mg/L)	6.00	8.79	5.00
Conductivity (mg/L)	600.00	9.57	-
pH	2.39	6.70	5.00–9.00

It was important make sure that the pH value after the reduction process and before neutralization was 2.78. In addition, after application, pyritic waste was leached with water for 24 h in the same system and kept at rest inside the column for 7 days to promote new oxidation on the pyrite surfaces and provide a new use for the chromium treatment process.

4. Conclusions

Pyrite oxidation is a natural reaction that involves water, oxygen, sulfur oxidation, and a species that can be reduced to iron. Reduction in the pyrite system is well-known and is responsible for AMD generation, causing environmental damage. However, if the system is applied in a controlled manner, pyrite can be used as an industrial reagent to treat hexavalent chromium wastewater.

The system reduction development was based on natural reactions, where a pyrite concentrate produced in coal mining was "dissolved" by hexavalent chromium, based on electrochemical interactions on the surface of pyrite with metallic ions in solution. As the electrochemical potential of hexavalent chromium is stronger than iron, the chromium is reduced first and released into the solution as iron, which acts as a chemical coagulant to promote the reduction of the metallic contents in the wastewater.

The sludge obtained by the treatment system, after being dried, ground, and calcined, had mineralogical characteristics and colour properties similar to pigments applied in the ceramic industry. However, the chemical compositions and particle sizes were different because sources of chromium, iron, and zinc were not controlled and the milling process was less effective, both of which factors have great impacts on colour and dispersion in ceramic applications.

The treated effluent showed total neutralization of hexavalent chromium, i.e., the concentration of the main hazardous component (Cr^{6+}) was below the amount detectable by standard methods for the examination of water and wastewater [63]. Trivalent chromium was found to have a concentration of 0.8 mg/L in the effluent—less than the 1.0 mg/L maximum limit required by environmental legislation (CONAMA 430/2011). Additionally, the effluent generated had characteristics of low turbidity, colourlessness, and a pH close to neutral (pH: 6.70). Thus, the effluent could be discharged into the environment without causing damage [76].

One of the disadvantages of the process is that the pyrite loses its reduction efficiency, requiring time to breathe; that is, after the treatment of a certain amount of effluent, the pyrite saturates, losing its power of reduction, and has to be exposed to the air for natural oxidation to occur. Future process optimization is needed, in which the pyrite saturation times and characterizations of the same must be determined; the influence of parameters (effluent flow rate, pH variation, Cr concentration variations, among others) on pigment generation must be determined; the cost of the process should be evaluated in more detail; and, finally, a business plan must be developed and scaled up.

Author Contributions: Conceptualization, R.d.A.S., J.C.S.d.S.M. and I.A.H.S.; data curation, M.P.S. and R.T.L.; formal analysis, R.d.A.S. and M.P.S.; investigation, R.d.A.S. and M.P.S.; methodology, M.P.S.; project administration, R.d.A.S.; resources, R.T.L.; validation, J.C.S.d.S.M.; visualization, J.C.S.d.S.M., I.A.H.S. and R.T.L.; writing—original draft preparation, R.d.A.S.; writing—review and editing, I.A.H.S. and R.T.L. All authors have read and agreed to the published version of the manuscript.

Funding: This research received no external funding.

Institutional Review Board Statement: Not applicable.

Informed Consent Statement: Not applicable.

Data Availability Statement: The data presented in this study are available upon reasonable request from the corresponding author.

Acknowledgments: The authors would like to thank the Fundação Meridional, CNPq, Cambuí, Laprom-UFRG, Satic-CNTCL for the grant of financial and technical support.

Conflicts of Interest: The authors declare no conflict of interest.

References

1. Weiler, J.; Firpo, B.A.; Schneider, I.A.H. Coal Waste Derived Soil-like Substrate: An Opportunity for Coal Waste in a Sustainable Mineral Scenario. *J. Clean. Prod.* **2018**, *174*, 739–745. [CrossRef]
2. Bi, G.; Shao, Y.; Song, W.; Yang, F.; Luo, Y. A Performance Evaluation of China's Coal-Fired Power Generation with Pollutant Mitigation Options. *J. Clean. Prod.* **2018**, *171*, 867–876. [CrossRef]
3. Bian, Z.; Dong, J.; Lei, S.; Leng, H.; Mu, S.; Wang, H. The Impact of Disposal and Treatment of Coal Mining Wastes on Environment and Farmland. *Environ. Geol.* **2009**, *58*, 625–634. [CrossRef]
4. Oliveira, C.M.; Machado, C.M.; Duarte, G.W.; Peterson, M. Beneficiation of Pyrite from Coal Mining. *J. Clean. Prod.* **2016**, *139*, 821–827. [CrossRef]
5. Yang, Y.; Zheng, X.; Sun, Z. Coal Resource Security Assessment in China: A Study Using Entropy-Weight-Based TOPSIS and BP Neural Network. *Sustainability* **2020**, *12*, 2294. [CrossRef]
6. Komnitsas, K.; Paspaliaris, I.; Zilberchmidt, M.; Groudev, S. Environmental Impacts at Coal Waste Disposal Sites-Efficiency of Desulfurization Technologies. *Glob. Nest Int. J.* **2001**, *3*, 135–142.
7. Zhao, Q.; Guo, F.; Zhang, Y.; Ma, S.; Jia, X.; Meng, W. How Sulfate-Rich Mine Drainage Affected Aquatic Ecosystem Degradation in Northeastern China, and Potential Ecological Risk. *Sci. Total Environ.* **2017**, *609*, 1093–1102. [CrossRef]
8. Burmistrz, P.; Kogut, K.; Marczak, M.; Dziok, T.; Górecki, J. Mercury in Polish Coking Bituminous Coals. *Energy Fuels* **2018**, *32*, 5677–5683. [CrossRef]
9. Krūmiņš, J.; Kļaviņš, M.; Ozola-Davidāne, R.; Ansone-Bērtiņa, L. The Prospects of Clay Minerals from the Baltic States for Industrial-Scale Carbon Capture: A Review. *Minerals* **2022**, *12*, 349. [CrossRef]
10. Amaral Filho, J.R.D.; Schneider, I.A.H.; de Brum, I.A.S.; Sampaio, C.H.; Miltzarek, G.; Schneider, C. Characterization of a Coal Tailing Deposit for Integrated Mine Waste Management in the Brazilian Coal Field of Santa Catarina. *Rem Rev. Esc. Minas* **2013**, *66*, 347–353. [CrossRef]
11. Nie, J.; Kuang, L.; Li, Z.; Xu, W.; Cheng, W.; Chen, Q.; An, L.I.; Zhao, X.; Xie, H.; Zhao, D. Assessing the Concentration and Potential Health Risk of Heavy Metals in China's Main Deciduous Fruits. *J. Integr. Agric.* **2016**, *15*, 1645–1655. [CrossRef]
12. Keith, M.; Smith, D.J.; Jenkin, G.R.T.; Holwell, D.A.; Dye, M.D. A Review of Te and Se Systematics in Hydrothermal Pyrite from Precious Metal Deposits: Insights into Ore-Forming Processes. *Ore Geol. Rev.* **2018**, *96*, 269–282. [CrossRef]
13. Berner, R.A. Sedimentary Pyrite Formation: An Update. *Geochim. Cosmochim. Acta* **1984**, *48*, 605–615. [CrossRef]
14. Akcil, A.; Koldas, S. Acid Mine Drainage (AMD): Causes, Treatment and Case Studies. *J. Clean. Prod.* **2006**, *14*, 1139–1145. [CrossRef]
15. Simate, G.S.; Ndlovu, S. Acid Mine Drainage: Challenges and Opportunities. *J. Environ. Chem. Eng.* **2014**, *2*, 1785–1803. [CrossRef]
16. Skousen, J.G.; Ziemkiewicz, P.F.; McDonald, L.M. Acid Mine Drainage Formation, Control and Treatment: Approaches and Strategies. *Extr. Ind. Soc.* **2019**, *6*, 241–249. [CrossRef]
17. Moreno-González, R.; Macías, F.; Olías, M.; Cánovas, C.R. Temporal Evolution of Acid Mine Drainage (AMD) Leachates from the Abandoned Tharsis Mine (Iberian Pyrite Belt, Spain). *Environ. Pollut.* **2022**, *295*, 118697. [CrossRef]
18. Kim, J.; Jung, P.-K.; Moon, H.-S.; Chon, C.-M. Reduction of Hexavalent Chromium by Pyrite-Rich Andesite in Different Anionic Solutions. *Environ. Geol.* **2002**, *42*, 642–648. [CrossRef]
19. Vigânico, E.M.; Colling, A.V.; de Almeida Silva, R.; Schneider, I.A.H. Biohydrometallurgical/UV Production of Ferrous Sulphate Heptahydrate Crystals from Pyrite Present in Coal Tailings. *Miner. Eng.* **2011**, *24*, 1146–1148. [CrossRef]
20. Kontopoulos, A.; Castro, S.H.; Vergara, F.; Sánchez, M.A. Acid Mine Drainage Control, Effluent Treatment in the Mining Industry. *Univ. Concepción–Chile* **1998**, *57*, 75.
21. Evangelou, V.P.; Zhang, Y.L. A Review: Pyrite Oxidation Mechanisms and Acid Mine Drainage Prevention. *Crit. Rev. Environ. Sci. Technol.* **1995**, *25*, 141–199. [CrossRef]
22. Rosso, K.M. Structure and Reactivity of Semiconducting Mineral Surfaces: Convergence of Molecular Modeling and Experiment. *Rev. Miner. Geochem.* **2001**, *42*, 199–271. [CrossRef]
23. Rimstidt, J.D.; Vaughan, D.J. Pyrite Oxidation: A State-of-the-Art Assessment of the Reaction Mechanism. *Geochim. Cosmochim. Acta* **2003**, *67*, 873–880. [CrossRef]
24. Concer, P.H.; de Oliveira, C.M.; Montedo, O.R.K.; Angioletto, E.; Peterson, M.; Fiori, M.A.; Moreira, R. Kinetics of the Oxidation Reactions and Decomposition of Pyrite. *Cerâmica* **2017**, *63*, 39–43. [CrossRef]
25. Kim, T.B.; Choi, J.W.; Ryu, H.S.; Cho, G.B.; Kim, K.W.; Ahn, J.H.; Cho, K.K.; Ahn, H.J. Electrochemical Properties of Sodium/Pyrite Battery at Room Temperature. *J. Power Sources* **2007**, *174*, 1275–1278. [CrossRef]
26. Strauss, E.; Ardel, G.; Livshits, V.; Burstein, L.; Golodnitsky, D.; Peled, E. Lithium Polymer Electrolyte Pyrite Rechargeable Battery: Comparative Characterization of Natural Pyrite from Different Sources as Cathode Material. *J. Power Sources* **2000**, *88*, 206–218. [CrossRef]
27. Min, X.; Li, Q.; Zhang, X.; Liu, L.; Xie, Y.; Guo, L.; Liao, Q.; Yang, Z.; Yang, W. Characteristics, Kinetics, Thermodynamics and Long-Term Effects of Zerovalent Iron/Pyrite in Remediation of Cr (VI)-Contaminated Soil. *Environ. Pollut.* **2021**, *289*, 117830. [CrossRef]
28. Benincasa, E.; Brigatti, M.F.; Franchini, G.; Malferrari, D.; Medici, L.; Poppi, L.; Tonelli, M. Reactions between Cr (VI) Solutions and Pyrite: Chemical and Surface Studies. *Geol. Carpathica* **2002**, *53*, 79–85.

29. Zouboulis, A.I.; Kydros, K.A.; Matis, K.A. Arsenic (III) and Arsenic (V) Removal from Solutions by Pyrite Fines. *Sep. Sci. Technol.* **1993**, *28*, 2449–2463. [CrossRef]
30. Houda, Z.; Wang, Q.; Wu, Y.; Xu, X. Reduction Remediation of Hexavalent Chromium by Pyrite in the Aqueous Phase. *J. Appl. Sci.* **2007**, *7*, 1522–1527. [CrossRef]
31. Lu, A.; Zhong, S.; Chen, J.; Shi, J.; Tang, J.; Lu, X. Removal of Cr (VI) and Cr (III) from Aqueous Solutions and Industrial Wastewaters by Natural Clino-Pyrrhotite. *Environ. Sci. Technol.* **2006**, *40*, 3064–3069. [CrossRef] [PubMed]
32. Kantar, C.; Ari, C.; Keskin, S.; Dogaroglu, Z.G.; Karadeniz, A.; Alten, A. Cr (VI) Removal from Aqueous Systems Using Pyrite as the Reducing Agent: Batch, Spectroscopic and Column Experiments. *J. Contam. Hydrol.* **2015**, *174*, 28–38. [CrossRef] [PubMed]
33. Luz, A.B.D.; Lins, F.A.F. *Rochas & Minerais Industriais: Usos e Especificações*; CETEM/MCT: Rio de Janeiro, Brazil, 2008.
34. Kapoor, R.T.; Mfarrej, M.F.B.; Alam, P.; Rinklebe, J.; Ahmad, P. Accumulation of Chromium in Plants and Its Repercussion in Animals and Humans. *Environ. Pollut.* **2022**, *301*, 119044. [CrossRef] [PubMed]
35. Ober, J.A. *Mineral Commodity Summaries 2016*; US Geological Survey: Reston, VA, USA, 2016.
36. Kumari, B.; Tiwary, R.K.; Srivastava, K.K. Physico-Chemical Analysis and Correlation Study of Water Resources of the Sukinda Chromite Mining Area, Odisha, India. *Mine Water Environ.* **2017**, *36*, 356–362. [CrossRef]
37. Murthy, Y.R.; Tripathy, S.K.; Kumar, C.R. Chrome Ore Beneficiation Challenges & Opportunities–a Review. *Miner. Eng.* **2011**, *24*, 375–380.
38. Barnhart, J. Occurrences, Uses, and Properties of Chromium. *Regul. Toxicol. Pharmacol.* **1997**, *26*, S3–S7. [CrossRef]
39. Fazzo, L.; Minichilli, F.; Santoro, M.; Ceccarini, A.; della Seta, M.; Bianchi, F.; Comba, P.; Martuzzi, M. Hazardous Waste and Health Impact: A Systematic Review of the Scientific Literature. *Environ. Health* **2017**, *16*, 1–11. [CrossRef]
40. Lunk, H.-J. Discovery, Properties and Applications of Chromium and Its Compounds. *ChemTexts* **2015**, *1*, 1–17. [CrossRef]
41. Koleli, N.; Demir, A. Chromite. In *Environmental Materials and Waste: Resource Recovery and Pollution Prevention*; Academic Press: Cambridge, MA, USA, 2016; ISBN 012803906X.
42. Della, V.P.; Junkes, J.A.; Kuhn, I.; Hiella, H.G.; Hotza, D. Utilização Do Subproduto Da Recuperação Metálica de Escórias de Aços Inoxidáveis Na Síntese de Pigmentos Cerâmicos; Caracterização Da Matéria-Prima. *Cerâmica* **2005**, *51*, 111–116. [CrossRef]
43. GracePavithra, K.; Jaikumar, V.; Kumar, P.S.; SundarRajan, P. A Review on Cleaner Strategies for Chromium Industrial Wastewater: Present Research and Future Perspective. *J. Clean. Prod.* **2019**, *228*, 580–593. [CrossRef]
44. Beukes, J.P.; du Preez, S.P.; van Zyl, P.G.; Paktunc, D.; Fabritius, T.; Päätalo, M.; Cramer, M. Review of Cr (VI) Environmental Practices in the Chromite Mining and Smelting Industry–Relevance to Development of the Ring of Fire, Canada. *J. Clean. Prod.* **2017**, *165*, 874–889. [CrossRef]
45. McLean, J.E.; McNeill, L.S.; Edwards, M.A.; Parks, J.L. Hexavalent Chromium Review, Part 1: Health Effects, Regulations, and Analysis. *J.-Am. Water Work. Assoc.* **2012**, *104*, E348–E357. [CrossRef]
46. Tiwari, A.K.; Orioli, S.; de Maio, M. Assessment of Groundwater Geochemistry and Diffusion of Hexavalent Chromium Contamination in an Industrial Town of Italy. *J. Contam. Hydrol.* **2019**, *225*, 103503. [CrossRef]
47. Jin, W.; Du, H.; Zheng, S.; Zhang, Y. Electrochemical Processes for the Environmental Remediation of Toxic Cr (VI): A Review. *Electrochim. Acta* **2016**, *191*, 1044–1055. [CrossRef]
48. Liu, C.; Fiol, N.; Poch, J.; Villaescusa, I. A New Technology for the Treatment of Chromium Electroplating Wastewater Based on Biosorption. *J. Water Process Eng.* **2016**, *11*, 143–151. [CrossRef]
49. Ye, Z.; Yin, X.; Chen, L.; He, X.; Lin, Z.; Liu, C.; Ning, S.; Wang, X.; Wei, Y. An Integrated Process for Removal and Recovery of Cr (VI) from Electroplating Wastewater by Ion Exchange and Reduction–Precipitation Based on a Silica-Supported Pyridine Resin. *J. Clean. Prod.* **2019**, *236*, 117631. [CrossRef]
50. Qin, G.; McGuire, M.J.; Blute, N.K.; Seidel, C.; Fong, L. Hexavalent Chromium Removal by Reduction with Ferrous Sulfate, Coagulation, and Filtration: A Pilot-Scale Study. *Environ. Sci. Technol.* **2005**, *39*, 6321–6327. [CrossRef]
51. Kaprara, E.; Simeonidis, K.; Zouboulis, A.I.; Mitrakas, M. Evaluation of Current Treatment Technologies for Cr (VI) Removal from Water Sources at Sub-Ppb Levels. In Proceedings of the 13th International Conference on Environmental Science and Technology, Athens, Greece, 5–7 September 2013; pp. 5–7.
52. Fu, F.; Cheng, Z.; Dionysiou, D.D.; Tang, B. Fe/Al Bimetallic Particles for the Fast and Highly Efficient Removal of Cr (VI) over a Wide PH Range: Performance and Mechanism. *J. Hazard. Mater.* **2015**, *298*, 261–269. [CrossRef]
53. Barrera-Díaz, C.E.; Lugo-Lugo, V.; Bilyeu, B. A Review of Chemical, Electrochemical and Biological Methods for Aqueous Cr (VI) Reduction. *J. Hazard. Mater.* **2012**, *223*, 1–12. [CrossRef]
54. Almeida, J.C.; Cardoso, C.E.D.; Tavares, D.S.; Freitas, R.; Trindade, T.; Vale, C.; Pereira, E. Chromium Removal from Contaminated Waters Using Nanomaterials–a Review. *TrAC Trends Anal. Chem.* **2019**, *118*, 277–291. [CrossRef]
55. Zeng, J.; Yue, Y.; Gao, Q.; Zhang, J.; Zhou, J.; Pan, Y.; Qian, G.; Tang, J.; Ruan, J. Co-Treatment of Hazardous Wastes by the Thermal Plasma to Produce an Effective Catalyst. *J. Clean. Prod.* **2019**, *208*, 243–251. [CrossRef]
56. Frondel, M.; Horbach, J.; Rennings, K. End-of-pipe or Cleaner Production? An Empirical Comparison of Environmental Innovation Decisions across OECD Countries. *Bus. Strategy Environ.* **2007**, *16*, 571–584. [CrossRef]
57. Gayo, G.X.; Lavat, A.E. Green Ceramic Pigment Based on Chromium Recovered from a Plating Waste. *Ceram. Int.* **2018**, *44*, 22181–22188. [CrossRef]
58. Pelino, M. Recycling of Zinc-Hydrometallurgy Wastes in Glass and Glass Ceramic Materials. *Waste Manag.* **2000**, *20*, 561–568. [CrossRef]

59. Garcia-Valles, M.; Avila, G.; Martinez, S.; Terradas, R.; Nogués, J.M. Heavy Metal-Rich Wastes Sequester in Mineral Phases through a Glass–Ceramic Process. *Chemosphere* **2007**, *68*, 1946–1953. [CrossRef] [PubMed]
60. Costa, G.; Ribeiro, M.J.; Trindade, T.; Labrincha, J.A. Development of Waste-Based Ceramic Pigments. *Bol. Soc. Esp. Ceram. Y Vidr.* **2007**, *46*, 7–13. [CrossRef]
61. Costa, G.; Della, V.P.; Ribeiro, M.J.; Oliveira, A.P.N.; Monrós, G.; Labrincha, J.A. Synthesis of Black Ceramic Pigments from Secondary Raw Materials. *Dye. Pigment.* **2008**, *77*, 137–144. [CrossRef]
62. Berry, F.J.; Costantini, N.; Smart, L.E. Synthesis of Chromium-Containing Pigments from Chromium Recovered from Leather Waste. *Waste Manag.* **2002**, *22*, 761–772. [CrossRef]
63. Abreu, M.A. de Reciclagem Do Resíduo de Cromo Da Indústria Do Curtume Como Pigmentos Cerâmicos. Ph.D. Thesis, Escola Politécnica da Universidade de São Paulo (USP), São Paulo, SP, Brasil, 2006.
64. Menezes, J.; Colling, A.V.; Silva, R.A.S.; dos Santos, R.H.; Scheneider, I.A.H. Ferric Sulphate Coagulant Obtained by Leaching from Coal Tailings. *Mine Water Environ.* **2017**, *36*, 457–460. [CrossRef]
65. Ozel, E.; Turan, S. Production and Characterisation of Iron-Chromium Pigments and Their Interactions with Transparent Glazes. *J. Eur. Ceram. Soc.* **2003**, *23*, 2097–2104. [CrossRef]
66. CONAMA Resolução 357/2005. 2005.
67. American Public Health Association. APHA Standard Methods for the Examination of Water and Wastewater. In *Standard Methods for the Examination of Water & Wastewater*; American Public Health Association: Washington, DC, USA, 2005.
68. Markiewicz, B.; Komorowicz, I.; Sajnóg, A.; Belter, M.; Barałkiewicz, D. Chromium and Its Speciation in Water Samples by HPLC/ICP-MS–Technique Establishing Metrological Traceability: A Review since 2000. *Talanta* **2015**, *132*, 814–828. [CrossRef] [PubMed]
69. Vogel, A.I. *A Text-Book of Macro and Semimicro Qualitative Inorganic Analysis*, 5th ed.; Svehla, G., Ed.; Longman: London, UK; New York, NY, USA, 1979; Volume 1.
70. *ASTM D7348-21*; Standard Test Methods for Loss on Ignition (LOI) of Solid Combustion Residues. EUA: West Conshohocken, PA, USA, 2021.
71. Liao, C.; Tang, Y.; Liu, C.; Shih, K.; Li, F. Double-Barrier Mechanism for Chromium Immobilization: A Quantitative Study of Crystallization and Leachability. *J. Hazard. Mater.* **2016**, *311*, 246–253. [CrossRef] [PubMed]
72. Li, B.; Chen, C.; Zhang, Y.; Yuan, L.; Deng, H.; Qian, W. Preparation of Glass-Ceramics from Chromite-Containing Tailings Solidified with Red Mud. *Surf. Interfaces* **2021**, *25*, 101210. [CrossRef]
73. Silva, R.d.A.; Petter, C.O.; Schneider, I.A.H. Avaliação Da Perda Da Coloração Artificial de Ágatas. *Rem Rev. Esc. Minas* **2007**, *60*, 477–482. [CrossRef]
74. Witt, K. CIE Guidelines for Coordinated Future Work on Industrial Colour-difference Evaluation. *Color Res. Appl.* **1995**, *20*, 399–403. [CrossRef]
75. Marcello, R.R.; Galato, S.; Peterson, M.; Riella, H.G.; Bernardin, A.M. Inorganic Pigments Made from the Recycling of Coal Mine Drainage Treatment Sludge. *J. Environ. Manag.* **2008**, *88*, 1280–1284. [CrossRef]
76. Burlakovs, J.; Jani, Y.; Kriipsalu, M.; Vincevica-Gaile, Z.; Kaczala, F.; Celma, G.; Ozola, R.; Rozina, L.; Rudovica, V.; Hogland, M. On the Way to 'Zero Waste'Management: Recovery Potential of Elements, Including Rare Earth Elements, from Fine Fraction of Waste. *J. Clean. Prod.* **2018**, *186*, 81–90. [CrossRef]